Structural Analysis of the SH3 Domain of β-PIX and Its Interaction with α-p21 Activated Kinase (PAK)[†,‡]

Helen R. Mott,* Daniel Nietlispach, Katrina A. Evetts, and Darerca Owen*

Department of Biochemistry, University of Cambridge, 80, Tennis Court Road, Cambridge, CB2 1GA U.K.

Received February 28, 2005; Revised Manuscript Received May 25, 2005

ABSTRACT: The PAK Ser/Thr kinases are important downstream effectors of the Rho family GTPases Cdc42 and Rac, partly mediating the role of these G proteins in cell proliferation and cytoskeletal rearrangements. As well as small G proteins, PAK interacts with the Cdc42/Rac exchange factor β-PIX via the PIX SH3 domain and a nontypical Pro-rich region in PAK. This interaction is thought to affect the localization of PAK, as well as increased GTP/GDP exchange of Rac and Cdc42. We have determined the structure of the PIX-SH3/PAK peptide complex and shown that it differs from typical Src-like SH3/peptide complexes. The peptide makes contacts through the Pro-rich sequence in a similar way to standard SH3/peptide complexes, even though the Pro residue positions are not conserved. In addition, there are interactions with a Pro and Lys in the PAK, which are C-terminal to the conserved Arg found in all SH3-binding sequences. These contact a fourth binding pocket on the SH3 domain. We have measured the affinity of PIX-SH3 for the PAK peptide and found that it is of intermediate affinity. When PAK is activated, Ser-199 in the PIX-binding site is phosphorylated. This phosphorylation is sufficient to reduce the affinity for PIX 6-fold.

Cdc42 and Rac are members of the Rho subfamily of small G proteins, which are involved in controlling changes in the actin cytoskeleton, regulating the formation of filopodia and lamellipodia, respectively (*1*). They have also been implicated in a variety of other signal transduction events, e.g., activation of transcription, cell cycle progression, and vesicle trafficking (*2*, *3*). Many of the effects of Cdc42 and Rac have been ascribed to the downstream Ser/Thr kinase PAK (p21-activated kinase).[1] PAK is thought to function in regulation of the cytoskeleton, activation of MAP kinase pathways, cell cycle progression, apoptotic signaling, and HIV infection (reviewed in refs *4* and *5*). The activation of this kinase is likely to be tightly controlled, and it appears to be regulated at several levels, including dimerization, localization, and binding of active G proteins (*6*).

At present six isoforms of PAK have been isolated, the best studied being PAK1 and PAK3. These PAKs contain a G protein binding domain (GBD) near their N-terminus, which contains the CRIB (Cdc42/Rac interaction and binding) consensus (*7*). This GBD overlaps with a kinase inhibitory domain (KID), which negatively regulates the kinase in the absence of stimulation (*8*−*11*). It was first thought that this simple switch controlled PAK activity in vivo, but this view has been complicated by recent work that indicates a more complex mechanism of PAK activation.

The NMR structure of the Cdc42/GBD complex has been solved (*12*), as well as a crystal structure of the GBD/KID regions in complex with the kinase domain (*13*). These show that parts of the GBD, notably a β-hairpin and an α-helix, adopt the same structure in the autoinhibited (kinase-bound) and activated (Cdc42-bound) forms. These elements pack against either Cdc42 or the KID/kinase, mainly through hydrophobic contacts: this implies that there may be some local unfolding involved in the activation mechanism, as one set of interactions is substituted for another. The crystal structure of the GBD/KID/kinase complex also revealed that the autoinhibited form of PAK exists as a dimer, with the dimerization mediated by the GBD and parts of the KID. Furthermore, it was shown, using coexpression of two different PAK mutants that could not form the intramolecular, autoinhibition interactions, that the KID from one molecule interacts with the kinase domain from another, i.e., that the PAK1 homodimers can be autoinhibited in trans (*14*) and are arranged in a head-to-tail fashion. The effects of Cdc42 binding on PAK dimerization are controversial: size exclusion chromatography data suggested that the PAK dimer is maintained both in the Cdc42 complex with PAK (57−200) and with full-length PAK (*15*), while co-immunoprecipitation studies implied that activated Cdc42 inhibits formation of PAK homodimers (*14*).

As well as the GBD, KID, and kinase domain, PAK contains conventional SH3-binding motifs. One of them

[†] This work is a contribution from the Cambridge Centre for Molecular Recognition, which is supported by the Biotechnology and Biological Sciences Research Council and the Wellcome Trust. This work was supported by a Career Development Award from the Medical Research Council (to H.R.M.) and Project Grants from Cancer Research U.K. (C1465/A2590 and C11309/A5148).

[‡] The coordinates of the PIX-SH3/PAK peptide complex structure have been submitted to the RCSB Protein Data Bank, accession number 1ZSG.

* Address correspondence to H.R.M. or D.O. Tel: 44-1223-764825. Fax: 44-1223-766002. E-mail: mott@bioc.cam.ac.uk; do@bioc.cam.ac.uk.

[1] Abbreviations: PAK, p21-activated kinase; GBD, GTPase binding domain; KID, kinase inhibitory domain; HSQC, heteronuclear single-quantum correlation; NOE, nuclear Overhauser effect; NOESY, NOE spectroscopy; TOCSY, total correlation spectroscopy; GST, glutathione *S*-transferase.

10.1021/bi050374a CCC: $30.25
Published on Web 07/29/2005

interacts with the adaptor protein Nck, which is thought to be involved in recruiting PAK to the plasma membrane and may be involved in cell adhesion (reviewed in refs *4* and *5*). The PIX (or Cool) proteins contain an SH3 domain that binds with high affinity to a nonconventional SH3-binding motif (*16*, *17*). In addition to the SH3 domain, PIX contains Dbl homology and PH domains, which are usually present in guanine nucleotide exchange factors for the Rho family. The effects of the PAK/PIX interaction are under intense investigation and may be crucial to the role of PAK in signaling, for example, its involvement in MAP kinase activation (*18*). It appears that the downstream effects of PAK can be divided into kinase-mediated and kinase-independent pathways (*11*) and that PIX binding may be involved in both. PIX is thought to be tightly associated in an oligomeric complex with the protein GIT1 (*19*, *20*), also known as PKL (for paxillin kinase linker) (*21*) and Cat (*22*). GIT1 contains a GAP domain for the Arf small GTPase along with two paxillin-binding domains. This tyrosine-phosphorylated protein can thus interact with paxillin, a protein found in focal adhesions (*23*). One of the consequences of the PAK/PIX interaction is likely to be the localization of PAK to these sites of integrin interaction with the extracellular matrix. In addition, the PAK/PIX interaction may have other effects than simply localization. PIX is itself a dimer, and it appears that dimeric PIX is an exchange factor for Rac only in vivo (*17*). It has recently been reported, however, that binding to a complex of PAK and the $\beta\gamma$ subunits of heterotrimeric G proteins breaks up the PIX monomer and allows it to behave as an exchange factor for both Cdc42 and Rac (*24*). It has been reported that the PIX/PAK interaction can lead to both stimulation of the PIX exchange activity and activation of the PAK kinase (*25*), although this seems to be dependent on the isoform of PIX that is bound (*16*). The mechanisms of activation of these proteins by this interaction have not been determined. It has also been shown that PAK autophosphorylation is stimulated by GIT1 in a mechanism that is independent of Cdc42 and Rac binding (*26*).

More recently, it has been found that the E3 ubiquitin ligase Cbl proteins associate with β-PIX via the PIX SH3 domain and thus compete with PAK (*27*). This interaction is thought to sequester Cbl and protect EGF from ubiquitin-mediated degradation (*28*). The Pro-rich sequence of Cbl that binds to PIX-SH3 has not been fully delineated, but there is no obvious homology to the PAK atypical sequence.

We set out to investigate in more detail the interaction between PIX and PAK. We have determined the structure of the complex of the PIX-SH3 domain with the unconventional Pro-rich peptide from PAK, and we show that their interaction is different from the canonical Src SH3/peptide complexes. We also show that phosphorylation of Ser-199 of PAK decreases the affinity between PIX-SH3 and the PAK peptide 6-fold.

EXPERIMENTAL PROCEDURES

Protein Purification. The SH3 domain of β-PIX (residues 1−65) was expressed as a His-tagged protein in *Escherichia coli* BL21(DE3) harboring the expression construct. Labeled protein was produced by growing *E. coli* in a medium based on MOPS buffer, containing appropriately labeled 5% Celtone, $^{15}NH_4Cl$, and/or [^{13}C]glucose (Spectra Stable Isotopes). The fusion protein was affinity purified on a Ni^{2+}-NTA column (Qiagen) and cleaved from the His tag with factor Xa (Roche), followed by gel filtration on a Superdex-30 column (Amersham Biosciences), running in NMR buffer (20 mM Na_2HPO_4/NaH_2PO_4, pH 7.3, 100 mM Na_2SO_4, 0.05% NaN_3). The SH3 domain was concentrated to ca. 1.0 mM, and lyophilized peptide was added to make a 1:1 complex for NMR. The peptide corresponding to residues 183−204 of human α-PAK (native or phosphorylated at Ser-199) was purchased from MWG Biotech or Dr. G. Blomberg (University of Bristol, U.K.).

NMR Spectroscopy. NMR spectra were recorded at 25 °C on a Bruker DRX600 spectrometer, except for ^{13}C-separated NOESY, ^{13}C,^{15}N-filtered, ^{13}C-separated NOESY, and ^{13}C,^{15}N-rejected NOESY experiments, which were recorded on a Bruker DRX800. ^{15}N HSQC, ^{15}N-separated NOESY (120 ms mixing time), ^{15}N-separated TOCSY (47.4 ms DIPSI-2 mixing), HNHA, 2D ^{1}H-TOCSY (60.2 ms DIPSI-2 mixing), and 2D ^{1}H-NOESY (150 ms mixing) experiments were recorded on ^{15}N-labeled SH3 complexed with unlabeled peptide. HNCA, HN(CO)CA, HNCACB, CBCA(CO)NH, HNCO, (H)CC(CO)NH, (H)CCH-COSY, ^{13}C-HSQC, ^{13}C-separated NOESY (100 ms mixing time), ^{13}C,^{15}N-rejected, ^{13}C,^{15}N-separated NOESY (150 ms mixing time), doubly rejected ^{13}C,^{15}N NOESY (150 ms mixing), and TOCSY (30.5 ms mixing time) experiments were recorded on ^{15}N,^{13}C-labeled SH3 complexed with unlabeled peptide (see ref *29* and references cited therein). $^3J_{HN-H\alpha}$ couplings were measured using the HNHA experiment (*30*). Backbone torsion angles were estimated from CA, CO, CB, N, and HA chemical shifts using the program TALOS (*31*). NMR data were processed using the AZARA package and analyzed using ANSIG (*32*).

Structure Calculation. Structures were calculated iteratively, using CNS 1.0 and ARIA 1.0 (*33*), where the ambiguity of NOEs is reduced for each iteration by comparing the ambiguous NOE tables against the lowest energy structures from the previous iteration. Twenty structures were calculated for each iteration, and seven were used for ARIA analysis. The total contribution of the accepted NOEs to the volume of the cross-peak was reduced during the calculation from 1.0 to 0.8. The parameters used for the calculation were essentially those described in ref *33*, except that the length of the high-temperature dynamics was increased to 45 ps and the cooling to a total of 39 ps. The structures were directly refined against the $^3J_{HN-H\alpha}$ coupling constants (*34*). The ϕ and ψ restraints from TALOS were included with errors of ±30°, or twice the standard deviation, whichever was greater.

Fluorescence Spectroscopy. Fluorescence experiments were performed on a Perkin-Elmer LS 55 luminescence spectrometer at 23 °C. The excitation wavelength used was 280 nm, and the emission spectra were recorded from 300 to 400 nm. SH3 (1 μM) in a 1 mL cuvette was used as the starting point of the titration. Peptides were added from a 2 mM (native peptide) or 7 mM (phosphopeptide) stock. In each case, the peptide stock contained 1 μM SH3 to prevent dilution of the fluorescent signal. Peptides were added in 1 μM aliquots (native) or 3.5 μM aliquots (phospho) until the fluorescent signal stopped changing. The fluorescence intensity maximum at 347.5 nm was plotted against the peptide

concentration and fitted to the equation:

$$F_i = F_0 + \frac{F_{min} - F_0}{2[S]}[[S] + [P] + K_d - \sqrt{([S] + [P] + K_d)^2 - 4[S][P]}]$$

where F_i = intensity at any point, F_0 = intensity of free SH3, F_{min} = minimum intensity, [S] = concentration of SH3, [P] = concentration of peptide, and K_d = dissociation constant.

RESULTS

β-PIX-SH3/α-PAK Structure. Backbone resonances of the SH3 domain in the complex were assigned using triple resonance methodology (reviewed in ref *29*). Side chain resonances of the SH3 were assigned using (H)CC(CO)NH, (H)CCH-COSY, and ^{15}N-edited TOCSY experiments. PAK peptide resonances were assigned using ^{13}C,^{15}N-rejected TOCSY and NOESY experiments, as well as homonuclear 2D TOCSY, NOESY, and DQF-COSY. NOEs were measured from the following spectra: ^{15}N-separated NOESY (512 NOEs); 2D ^{1}H−^{1}H NOESY (1845 NOEs); ^{13}C-separated NOESY (1553 NOEs); ^{13}C,^{15}N-filtered, ^{13}C-separated NOESY (31 NOEs).

Initial structures were calculated using 2549 NOE restraints (of which 761 were ambiguous and 1788 were unambiguous), 33 pairs of loose torsion angle restraints from TALOS, and 49 $^{3}J_{HN-H\alpha}$ couplings. After eight iterations, there were 1494 unambiguous NOEs and 172 ambiguous, nondegenerate NOEs. In the final structure calculation, 100 structures were calculated for each round and the 30 with the lowest energy selected for analysis.

The structure of the PIX-SH3/α-PAK peptide complex is well defined by the NMR data and has good covalent geometry (Table 1). The SH3 domain forms a regular SH3 fold, with a central five-stranded β-sandwich and a β-hairpin between strands 1 and 2 (the RT loop) (Figures 1 and 2). SH3 domain ligands are asymmetric and have been classified into class I and class II types, with the consensus sequences RxxPxxP and xPxxPxR, respectively (*35*). The α-PAK peptide binds as a class II ligand to an interface that is predominantly composed of hydrophobic residues in the RT loop and the loops between strands 2 and 3 and between strands 4 and 5 (Figures 1 and 3). The peptide used in this study was equivalent to α-PAK residues 183−204. The line widths and NOE patterns in the 2D spectra indicate that residues 183−185 and 200−204 are unstructured (data not shown). Resonances corresponding to residues 195−198 had larger line widths than the rest of the peptide. These residues are likely to be undergoing conformational exchange on a millisecond to microsecond time scale. These four residues are necessary for the high-affinity binding between PIX and α-PAK peptides: mutations of His-196 or Thr-197 or removal of residues 198−204 decreases the interaction to 30−40% that of wild type (*17*). Our NMR data show that residues 200−204 are highly flexible and that they do not make any interactions with the SH3 domain.

The α-PAK peptide does not form a left-handed PPII helix, as do many Pro-rich SH3-binding peptides. Rather, it is made up of three turns, comprising residues 186−189, 188−191, and 190−193. These turns are followed by a region that is less well defined in the structure (194−199), whose resonances are broader than the rest of the peptide (Figure 2). This region is also involved in the interaction. Pro-194 and Lys-198 both contact residues on the SH3 domain, It appears, however, that residues 195−197 do not make any interactions in the complex (Figures 2 and 3).

Table 1: Experimental Restraints and Structural Statistics

		⟨*SA*⟩[a]	⟨*SA*⟩$_c$[b]
no. of exptl restraints			
unambiguous	1788		
ambiguous	761		
dihedral restraints	33		
$^{3}J_{HNH\alpha}$ couplings	49		
coordinate precision			
RMSD of backbone atoms (8−63; 186−196) (Å)		0.83 ± 0.22	0.54
RMSD of heavy atoms (8−63; 186−196) (Å)		1.36± 0.26	1.05
RMSD from exptl restraints			
NOE distances (Å)		0.030 ± 0.004	0.030
TALOS dihedral angles (deg)		0.45 ± 0.085	0.47
$^{3}J_{HNH\alpha}$ couplings (Hz)		0.53 ± 0.031	0.51
RMSD from idealized geometry			
bonds (Å)		0.0026 ± 0.00021	0.0027
angles (deg)		0.38 ± 0.021	0.37
impropers (deg)		0.29 ± 0.018	0.28
final energy			
E_{L-J}[c] (kJ/mol)		−766.78 ± 13.12	−757.78
Ramachandran analysis			
residues in most favored regions (%)		70.6	68.5
residues in additionally allowed regions (%)		23.7	30.1
residues in generously allowed regions (%)		3.4	0.0
residues in disallowed regions (%)		2.2	1.4

[a] ⟨*SA*⟩ represents the average RMS deviations for the ensemble. [b] ⟨*SA*⟩$_c$ represents values for the structure that is closest to the mean. [c] The Lennard-Jones potential was not used at any stage in the refinement.

In several other SH3/peptide complexes, residues C-terminal to the conserved basic residue are required for high-affinity binding, due to their interaction with residues in the RT loop of the SH3 domain (Figure 1). The Csk SH3 domain binds to the PEP tyrosine phosphatase via a regular PXXPXR motif, but there are also two hydrophobic residues C-terminal to this, which increase both the affinity and specificity of the interaction (*36*). The Gads SH3 domain interacts with a peptide from SLP-76, which contains a motif that binds the SH3 domain in the same manner as xPxxPxR and a C-terminal RxxK motif (*37*). The p67^{phox} SH3 domain seems to require 20 residues C-terminal to the PxxP motif for high-affinity binding to p47^{phox} (*38*).

Effects of Phosphorylation on PIX-SH3/PAK Interactions. The interaction between PAK and both PIX and Nck is modulated by PAK phosphorylation, and it has been suggested that this allows PAK to be released from focal complexes and recycled to the cytoplasm (*39*). The PAK peptide we have used in this study includes two phosphorylation sites, at Ser-199 and Ser-204. Our NMR data show that Ser-199 is in closer contact with PIX-SH3, so that its phosphorylation is most likely to affect binding. We therefore investigated the effects of phosphorylation at this residue on the interaction between PIX-SH3 and the α-PAK peptide using the intrinsic fluorescence of the three SH3 Trp residues,

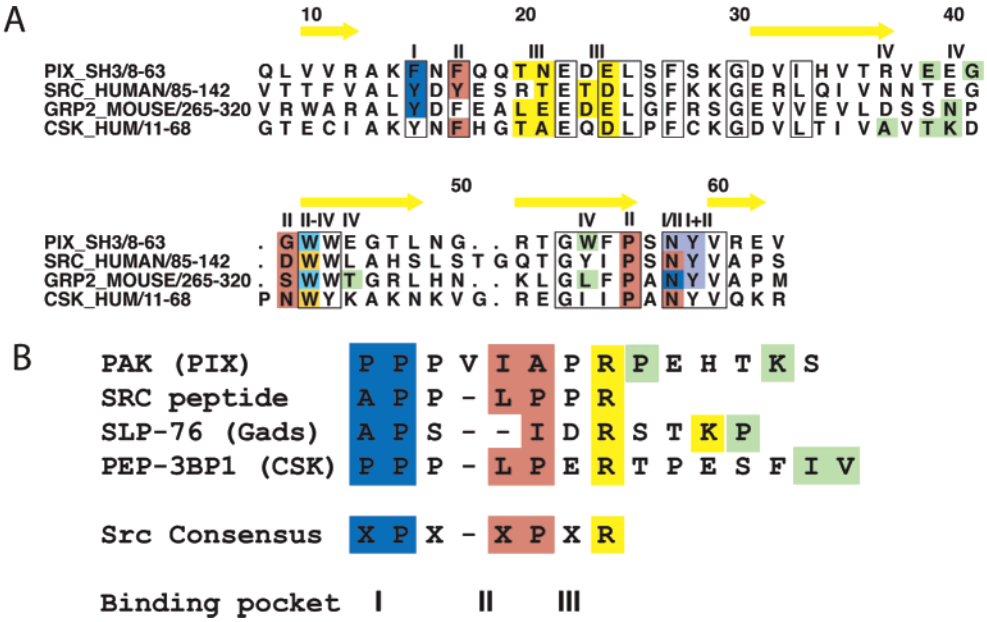

FIGURE 1: Sequence alignments showing the four binding pockets involved in the different types of SH3/peptide interactions. Conserved residues are boxed in all sequences. (A) The location of SH3 residues in the binding pockets are labeled I−IV above the sequences and colored as follows: pocket I, blue; pocket II, red; pocket III, yellow; pocket IV, green; pockets I and II, purple; pockets II and III, orange; pockets II, III, and IV, cyan. The residue numbering above the alignment is that of PIX-SH3. Yellow arrows denote the position of the β-strands in PIX-SH3. (B) The peptide-binding partners of the SH3 domains shown in (A), whose structures have been determined in complex with the SH3 domains. The residues that bind in the SH3-binding pockets shown in (A) are colored as follows: pocket I, blue; pocket II, red; pocket III, yellow; pocket IV, green. The canonical Src peptide consensus sequence is shown underneath the peptide sequences. This binds to only three pockets on the Src SH3 domain, and the residues responsible are indicated in the same colors.

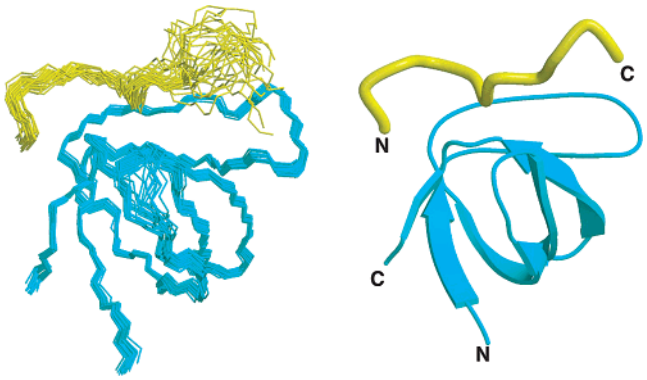

FIGURE 2: The PIX-SH3/PAK peptide structure. On the left are the lowest energy 30 structures (out of 100 calculated), and on the right is the structure that is closest to the mean. The PIX-SH3 domain is shown in cyan and the PAK peptide in yellow. Residues 8−63 of the SH3 domain and 186−196 of PAK are shown.

two of which are involved in the interaction with PAK (Figure 4A). The fluorescence maximum of free PIX-SH3 was at 347.5 nm, which decreased in intensity and blue shifted when the PAK peptide was added. The intensity at 347.5 nm was plotted against the total peptide concentration to evaluate the K_d. This gave an average K_d of 7.5 ± 0.3 μM. This value is higher than that measured previously by surface plasmon resonance with GST PIX-SH3 and GST PAK (183−204) (*17*). It is possible that the difference is due to the effects of GST dimerization, which could make the affinity appear higher. A value of 7.5 μM is closer to that expected for most SH3/peptide complexes (*35*). When the fluorescence titration was repeated with peptide that was phosphorylated at Ser-199, the measured K_d had increased to 43 ± 4 μM. Thus, the phosphorylation of the PAK peptide reduces the affinity for PIX-SH3 by 5.8-fold. This is consistent with data that show that PAK is no longer recruited

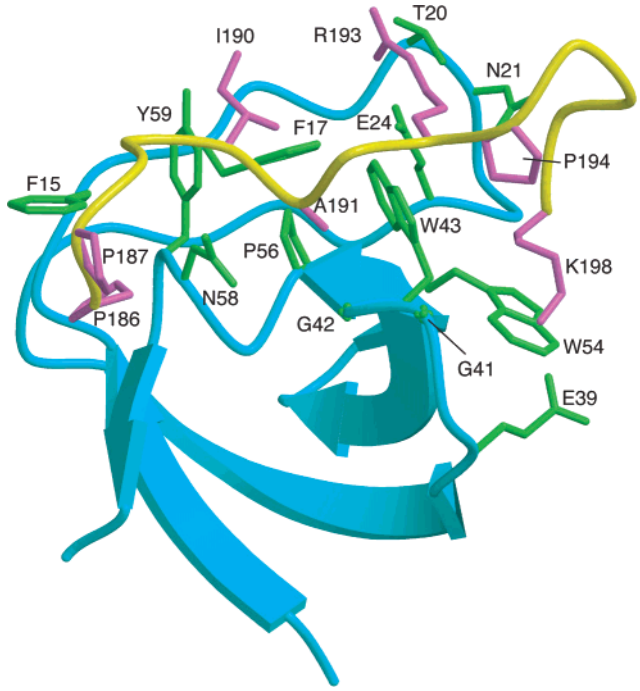

FIGURE 3: Side chains of PIX-SH3 and PAK peptide involved in the interaction. PIX-SH3 is shown in cyan with green side chains, and the PAK peptide is shown in yellow with violet side chains. The side chains are shown as sticks for clarity and are labeled with one-letter codes. Residues at the C-terminus of the PAK peptide are involved in the interaction with PIX-SH3, for example, Lys-198, which forms a salt bridge with Glu-39 of the SH3.

to GIT1/PIX complexes in vivo when it is phosphorylated (*39*). It was shown previously that mutation of Ser-199 to Glu, which could mimic the effect of phosphorylation, had only a small effect on the interaction with α-PIX, decreasing the affinity by 30% (*17*). The discrepancy between this and

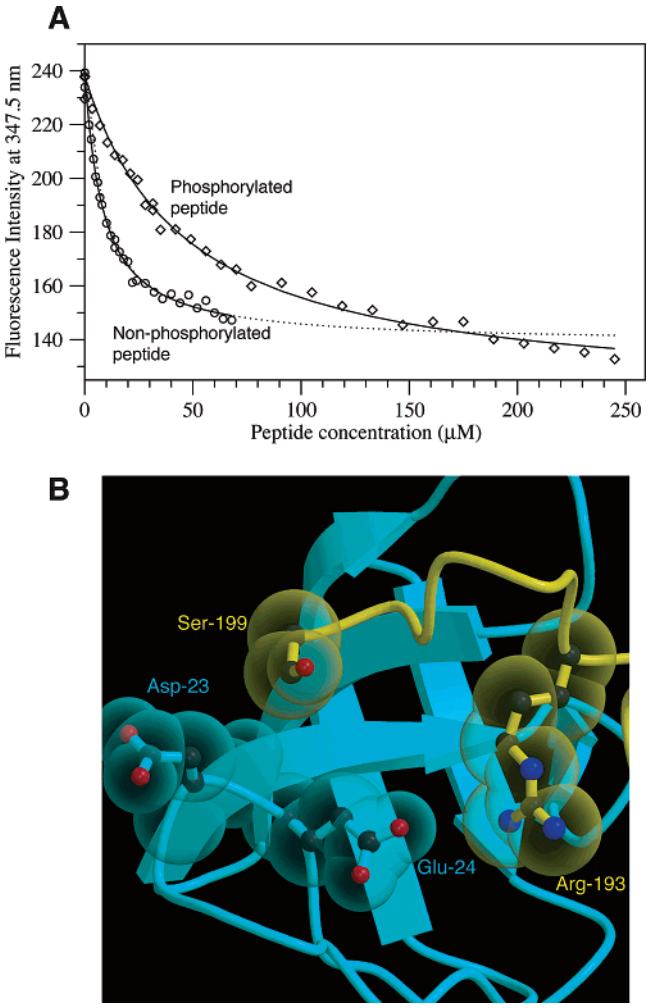

FIGURE 4: Effect of PAK peptide phosphorylation on the PIX-SH3 interaction. (A) Analysis of the PIX-SH3/PAK peptide interaction by steady-state fluorescence in the presence and absence of phosphorylation at Ser-199. The data shown are representative of three experiments. The fluorescence intensity at 347.5 nm (the intensity maximum of PIX-SH3) was plotted against the concentration of added peptide. The data were plotted and analyzed using GRAce. (B) Interaction of PAK Ser-199 with the PIX-SH3 domain. PIX-SH3 is shown in cyan, and the PAK peptide is shown in yellow. The side chains are depicted in a ball-and-stick representation, with the sticks in cyan and yellow, respectively, and the balls colored black (carbon), red (oxygen), or blue (nitrogen), overlaid with a semitransparent space-filling representation.

our results with phosphopeptide may be because mutation to Glu only introduces a single negative charge, while phosphorylation introduces two. Thus, the actual, in vivo modification is sufficient to change the affinity significantly.

Phosphorylation has been shown to regulate SH3/peptide interactions in other systems, for example, the Grb2/SH3 interaction with Sos (*40*). Interestingly, the interaction between PAK and Nck is also disrupted by phosphorylation, although in this case the phosphoserine is only three residues C-terminal to the conserved basic residue.

DISCUSSION

We have shown that PIX-SH3 binds to the α-PAK nontypical, Pro-rich peptide in a minus (or type II) orientation. The α-PAK does not form a left-handed PPII helix and makes contacts with the SH3 domain through four hydrophobic pockets on the surface of the SH3. The total buried surface area in the complex is 844.26 ± 89 Å^2, calculated over the structured regions of the SH3 (8−63) and peptide (186−199). The typical Src SH3/peptide complexes bind peptides with a lower affinity, with K_ds often more than 10 μM (*35*), and bury a smaller surface area (e.g., 665 Å^2 for Src/peptide: PDB code 1prl). The high-affinity SH3/peptide complexes, such as Gads/SLP-76 (K_d = 240 nM), bury a larger surface area (1017 Å^2: PDB code 1h3h). Thus, the PIX/PAK interaction is of intermediate affinity. One of the questions that remains to be answered about the various SH3/peptide complexes is how specificity is achieved when so many similar Pro-rich peptides exist that appear to bind multiple SH3 domains with essentially the same, relatively low, affinity. It is possible that PIX-SH3 would not bind to multiple peptides, since its mode of binding PAK is atypical, but this requires further investigation.

Like the SLP-76/Gads and Csk/PEP interactions, the PAK peptide binds PIX-SH3 via four pockets on the SH3 surface (Figure 3). The first of these pockets, lined by residues Phe-15, Asn-58, and Tyr-59, contacts Pro-186 and Pro-187, where Pro-187 is equivalent to the first "P" in the x-P-x-x-P-x-R sequence of a type II SH3-binding motif. Most of the contacts are made by Pro-186. The second hydrophobic pocket on the SH3 is composed of residues Phe-17, Gly-42, Trp-43, Pro-56, Asn-58, and Tyr-59 and is responsible for binding Ile-190 and Ala-191. Ala-191 is the residue equivalent to the second Pro in an x-P-x-x-P-x-R motif. Mutation of Ile-190 to Ala is sufficient to decrease the binding of the peptide to ∼20%, while mutation of Ala-191 to Gly only decreases the binding to ∼60% (*17*). The side chain of Ile-190 fits well into the pocket, making contacts with Phe-17, Trp-43, Pro-56, and Tyr-59. Replacement of the Ile-190 branched side chain with an Ala would leave a gap in this binding pocket, which is likely to be energetically unfavorable. The side chain of Ala-191, in contrast, contacts Gly-41, Gly-42, and Trp-43. It is possible that the presence of this pair of Gly residues means that replacement of the Ala methyl group with a proton (in the Ala → Gly mutant) can be accommodated by a reorientation of the SH3 main chain, explaining the lack of effect of the mutation. The third binding pocket on the SH3 is responsible for interacting with the conserved basic residue (Arg-193), which is present in all SH3-binding peptides. The pocket is lined by the side chains of Thr-20, Asn-21, Glu-24, and Trp-43, with the acidic residue in a position to make ionic interactions with the side chain of Arg-193. The fourth binding pocket in PIX-SH3 is atypical and is not observed in classical SH3 complexes, such as Src (*41*). In PIX-SH3, this pocket interacts with residues at the C-terminus of the PAK peptide, mainly Lys-198. The methylenes in the side chain of Lys-198 interact with a hydrophobic pocket lined by Trp-43, Trp54, and Gly-41, while the amine group makes a salt bridge with Glu-39. This pocket also buries part of Pro-194. Mutation of this Pro to Ala is also sufficient to decrease the binding of the peptide to ∼20% that of wild-type peptide (*17*). The Gads SH3 domain also has a hydrophobic pocket, in this case lined by Trp-300 (equivalent to Trp-43 in PIX) and Leu-311 (*37*). This pocket in Gads also interacts with a Pro residue in the SLP-76 peptide, which is in an analogous position to Pro-194 in the PAK peptide. Despite the similarity between the C-terminal ends of the SLP-76 and PAK peptides (a basic residue followed by a Pro), the remainder of the peptide

sequences are quite different: SLP-76 = APSIDRSTKP; PAK = PPPVIAPRPEHTKS. The PIX-SH3/PAK interaction thus has features in common with the RxxK motif SH3/peptide complexes, but it is also distinct.

Thus, the structure reveals that residues C-terminal to the Pro-rich core of the peptide are required for the interaction, for example, Lys-198, which makes an ionic interaction with Glu-39 of the SH3 domain. The interaction between this C-terminus and the fourth binding pocket contributes significantly to the affinity between PAK and PIX, since truncation of the peptide at Thr-197 decreased the affinity to ~30% (*17*). The importance of the C-terminus of this peptide is reinforced by the consequences of phosphorylation on peptide binding. We have quantified the effects of phosphorylation of Ser-199 of PAK in vitro and shown that it leads to a 6-fold decrease in the affinity between the PAK peptide and the PIX-SH3 domain. This change in affinity could be responsible for the lack of recruitment of PAK to GIT1/PIX complexes once it is activated and phosphorylated.

There were no intermolecular NOEs observed between Ser-199 and PIX-SH3 in our NMR spectra. Examination of the structure, however, shows that Ser-199 is close to an acidic patch on the surface of PIX-SH3 (Figure 4B) composed of the side chains of Asp-23 and Glu-24. Glu-24 makes a salt bridge with the side chain of Arg-193 in the PAK peptide. The effects of the addition of the phosphate group (and thus two negative charges) to Ser-199 are likely to be 2-fold. First, charge repulsion will cause Asp-23 and Glu-24 to be pushed away from the peptide, destabilizing the salt bridge between Glu-24 and Arg-193. This would lead to Arg-193 being free to form an intramolecular salt bridge with the phosphoserine. The overall effect will be a rearrangement of the charges in this region and the removal of one of the crucial intermolecular interactions.

The residues important for the interactions described here are conserved between the mammalian PAK isoforms 1−3 and the mammalian α- and β-PIX homologues. DPAK and the *Drosophila melanogaster* homologue of PIX also have these residues conserved, suggesting that this interaction is conserved. The *Caenorhabditis elegans* PAK/PIX homologues have several compensating changes compared to the human versions of the proteins. In CePAK, the equivalent residue to Pro-186 is a Val while Ala-191 is changed to a Pro. These residues are packed on either side of Asn-58 from PIX-SH3. In CePIX this Asn is changed to an Ala side chain, whose smaller size should compensate for the effect of the replacement of Ala-191 with a bulkier Pro. Interestingly, Lys-198 is replaced by a Leu in CePAK, so it can no longer form a salt bridge with Glu-39. Glu-39, strictly conserved in mammalian and *D. melanogaster* PIX-SH3s, is correspondingly replaced by its uncharged equivalent, Gln, in CePIX. The Leu equivalent in CePAK could still be partially buried by the residues equivalent to Trp-43 and Trp-54, which are conserved.

The PIX/PAK interaction between PIX-SH3 and the atypical Pro-rich peptide from PAK not only is important for PAK localization via the PIX/PKL interaction but also is implicated in PAK activation and nucleotide exchange of Rac and Cdc42. PAK activation leads to autophosphorylation of PAK at Ser-199, which then decreases the affinity for PIX. The PIX/PAK interaction thus drives PAK to cycle between focal complexes and the cytosol.

REFERENCES

1. Hall, A. (1998) Rho GTPases and the actin cytoskeleton, *Science 279*, 509−514.
2. Ridley, A. J. (2001) Rho family proteins: coordinating cell responses, *Trends Cell Biol. 11*, 471−477.
3. Olson, M. F., Ashworth, A., and Hall, A. (1995) An essential role for Rho, Rac, and Cdc42 Gtpases in cell-cycle progression through G(1), *Science 269*, 1270−1272.
4. Bagrodia, S., and Cerione, R. A. (1999) PAK to the future, *Trends Cell Biol. 9*, 350−355.
5. Daniels, R. H., and Bokoch, G. M. (1999) p21-activated protein kinase: a crucial component of morphological signaling?, *Trends Biochem. Sci. 24*, 350−355.
6. Bokoch, G. M. (2003) Biology of the p21-activated kinases, *Annu. Rev. Biochem. 72*, 743−781.
7. Burbelo, P. D., Drechsel, D., and Hall, A. (1995) A conserved binding motif defines numerous candidate target proteins for both Cdc42 and Rac GTPases, *J. Biol. Chem. 270*, 29071−29074.
8. Zhao, Z. S., Manser, E., Chen, X. Q., Chong, C., Leung, T., and Lim, L. (1998) A conserved negative regulatory region in alpha PAK: Inhibition of PAK kinases reveals their morphological roles downstream of Cdc42 and Rac1, *Mol. Cell. Biol. 18*, 2153−2163.
9. Zenke, F. T., King, C. C., Bohl, B. P., and Bokoch, G. M. (1999) Identification of a central phosphorylation site in p21-activated kinase regulating autoinhibition and kinase activity, *J. Biol. Chem. 274*, 32565−32573.
10. Tu, H., and Wigler, M. (1999) Genetic evidence for Pak1 autoinhibition and its release by Cdc42, *Mol. Cell. Biol. 19*, 602−611.
11. Frost, J. A., Khokhlatcheva, A., Stippec, S., White, M. A., and Cobb, M. H. (1998) Differential effects of PAK1-activating mutations reveal activity-dependent and -independent effects on cytoskeletal regulation, *J. Biol. Chem. 273*, 28191−28198.
12. Morreale, A., Venkatesan, M., Mott, H. R., Owen, D., Nietlispach, D., Lowe, P. N., and Laue, E. D. (2000) Structure of Cdc42 bound to the GTPase binding domain of PAK, *Nat. Struct. Biol. 7*, 384−388.
13. Lei, M., Lu, W. G., Meng, W. Y., Parrini, M. C., Eck, M. J., Mayer, B. J., and Harrison, S. C. (2000) Structure of PAK1 in an autoinhibited conformation reveals a multistage activation switch, *Cell 102*, 387−397.
14. Parrini, M. C., Lei, M., Harrison, S. C., and Mayer, B. J. (2002) Pak1 kinase homodimers are autoinhibited in trans and dissociated upon activation by Cdc42 and Rac1, *Mol. Cell 9*, 73−83.
15. Buchwald, G., Hostinova, E., Rudolph, M. G., Kraemer, A., Sickmann, A., Meyer, H. E., Scheffzek, K., and Wittinghofer, A. (2001) Conformational switch and role of phosphorylation in PAK activation, *Mol. Cell. Biol. 21*, 5179−5189.
16. Bagrodia, S., Taylor, S. J., Jordon, K. A., Van Aelst, L., and Cerione, R. A. (1998) A novel regulator of p21-activated kinases, *J. Biol. Chem. 273*, 23633−23636.
17. Manser, E., Loo, T. H., Koh, C. G., Zhao, Z. S., Chen, X. Q., Tan, L., Tan, I., Leung, T., and Lim, L. (1998) PAK kinases are directly coupled to the PIX family of nucleotide exchange factors, *Mol. Cell 1*, 183−192.
18. Lee, S. H., Eom, M., Lee, S. D., Kim, S., Park, H. J., and Park, D. (2001) beta Pix-enhanced p38 activation by Cdc42/Rac/PAK/MKK3/6-mediated pathway—Implication in the regulation of membrane ruffling, *J. Biol. Chem. 276*, 25066−25072.
19. Premont, R. T., Claing, A., Vitale, N., Freeman, J. L. R., Pitcher, J. A., Patton, W. A., Moss, J., Vaughan, M., and Lefkowitz, R. J. (1998) beta(2)-Adrenergic receptor regulation by GIT1, a G protein-coupled receptor kinase-associated ADP ribosylation factor GTPase-activating protein, *Proc. Natl. Acad. Sci. U.S.A. 95*, 14082−14087.
20. Premont, R. T., Perry, S. J., Schmalzigaug, R., Roseman, J. T., Xing, Y., and Claing, A. (2004) The GIT/PIX complex: an oligomeric assembly of GIT family ARF GTPase-activating proteins and PIX family Rac1/Cdc42 guanine nucleotide exchange factors, *Cell. Signalling 16*, 1001−1011.
21. Turner, C. E., Brown, M. C., Perrotta, J. A., Riedy, M. C., Nikolopoulos, S. N., McDonald, A. R., Bagrodia, S., Thomas, S., and Leventhal, P. S. (1999) Paxillin LD4 motif binds PAK and PIX through a novel 95-kD ankyrin repeat, ARF-GAP protein: A role in cytoskeletal remodeling, *J. Cell Biol. 145*, 851−863.
22. Bagrodia, S., Bailey, D., Lenard, Z., Hart, M., Guan, J. L., Premont, R. T., Taylor, S. J., and Cerione, R. A. (1999) A tyrosine-

phosphorylated protein that binds to an important regulatory region on the cool family of p21-activated kinase- binding proteins, *J. Biol. Chem. 274*, 22393−22400.
23. Brown, M. C., West, K. A., and Turner, C. E. (2002) Paxillin-dependent paxillin kinase linker and p21-activated kinase localization to focal adhesions involves a multistep activation pathway, *Mol. Biol. Cell 13*, 1550−1565.
24. Feng, Q. Y., Baird, D., and Cerione, R. A. (2004) Novel regulatory mechanisms for the Dbl family guanine nucleotide exchange factor Cool-2/alpha-Pix, *EMBO J. 23*, 3492−3504.
25. Daniels, R. H., Zenke, F. T., and Bokoch, G. M. (1999) alpha Pix stimulates p21-activated kinase activity through exchange factor-dependent and -independent mechanisms, *J. Biol. Chem. 274*, 6047−6050.
26. Loo, T. H., Ng, Y. W., Lim, L., and Manser, E. (2004) GITI activates p21-activated kinase through a mechanism independent of p21 binding, *Mol. Cell. Biol. 24*, 3849−3859.
27. Flanders, J. A., Feng, Q., Bagrodia, S., Laux, M. T., Singavarapu, A., and Cerione, R. A. (2003) The Cbl proteins are binding partners for the Cool/Pix family of p21-activated kinase-binding proteins, *FEBS Lett. 550*, 119−123.
28. Wu, W. J., Tu, S., and Cerione, R. A. (2003) Activated Cdc42 sequesters c-Cbl and prevents EGF receptor degradation, *Cell 114*, 715−725.
29. Ferentz, A. E., and Wagner, G. (2000) NMR spectroscopy: a multifaceted approach to macromolecular structure, *Q. Rev. Biophys. 33*, 29−65.
30. Vuister, G. W., and Bax, A. (1993) Quantitative J Correlation—a new approach for measuring homonuclear 3-bond J(H(N)H(Alpha) coupling-constants in N-15- enriched proteins, *J. Am. Chem. Soc. 115*, 7772−7777.
31. Cornilescu, G., Delaglio, F., and Bax, A. (1999) Protein backbone angle restraints from searching a database for chemical shift and sequence homology, *J. Biomol. NMR 13*, 289−302.
32. Kraulis, P. J., Domaille, P. J., Campbell-Burk, S. L., Van Aken, T., and Laue, E. D. (1994) Solution structure and dynamics of Ras P21·GDP determined by heteronuclear 3-dimensional and 4-dimensional NMR-spectroscopy, *Biochemistry 33*, 3515−3531.
33. Linge, J. P., O'Donoghue, S. I., and Nilges, M. (2001) Automated assignment of ambiguous NOEs with ARIA, *339*, 71−90.
34. Garrett, D. S., Kuszewski, J., Hancock, T. J., Lodi, P. J., Vuister, G. W., Gronenborn, A. M., and Clore, G. M. (1994) The impact of direct refinement against 3-bond Hn-C-Alpha-H coupling-constants on protein-structure determination by NMR, *J. Magn. Reson., Ser. B 104*, 99−103.
35. Mayer, B. J. (2001) SH3 domains: complexity in moderation, *J. Cell Sci. 114*, 1253−1263.
36. Ghose, R., Shekhtman, A., Goger, M. J., Ji, H., and Cowburn, D. (2001) A novel, specific interaction involving the Csk SH3 domain and its natural ligand, *Nat. Struct. Biol. 8*, 998−1004.
37. Liu, Q., Berry, D., Nash, P., Pawson, T., McGlade, C. J., and Li, S. S. C. (2003) Structural basis for specific binding of the gads SH3 domain to an RxxK motif-containing SLP-76 peptide: A novel mode of peptide recognition, *Mol. Cell 11*, 471−481.
38. Kami, K., Takeya, R., Sumimoto, H., and Kohda, D. (2002) Diverse recognition of non-PxxP peptide ligands by the SH3 domains from p67(phox), Grb2 and Pex13p, *EMBO J. 21*, 4268−4276.
39. Zhao, Z. S., Manser, E., and Lim, L. (2000) Interaction between PAK and Nck: a template for Nck targets and role of PAK autophosphorylation, *Mol. Cell. Biol. 20*, 3906−3917.
40. Zhao, H., Okada, S., Pessin, J. E., and Koretzky, G. A. (1998) Insulin receptor-mediated dissociation of Grb2 from Sos involves phosphorylation of Sos by kinase(s) other than extracellular signal-regulated kinase, *J. Biol. Chem. 273*, 12061−12067.
41. Feng, S. B., Kasahara, C., Rickles, R. J., and Schreiber, S. L. (1995) Specific interactions outside the proline-rich core of two classes of Src homology 3 ligands, *Proc. Natl. Acad. Sci. U.S.A. 92*, 12408−12415.

BI050374A